ELSEVIER

Biophysical Chemistry 104 (2003) 209–216

Biophysical Chemistry

www.elsevier.com/locate/bpc

# Ser-130 of *Natronobacterium pharaonis* halorhodopsin is important for the chloride binding

Maki Sato[a], Takashi Kikukawa[b], Tsunehisa Araiso[b], Hirotaka Okita[c], Kazumi Shimono[c], Naoki Kamo[c], Makoto Demura[a,*], Katsutoshi Nitta[a]

[a]*Division of Biological Sciences, Graduate School of Science, Hokkaido University, Sapporo 060-0810, Japan*
[b]*Center for Advanced Science and Technology, Hokkaido University, Sapporo 060-0810, Japan*
[c]*Graduate School of Pharmaceutical Sciences, Hokkaido University, Sapporo 060-0810, Japan*

Received 20 August 2002; received in revised form 12 November 2002; accepted 13 November 2002

**Abstract**

*Pharaonis* halorhodopsin (*p*hR) is an inward light-driven chloride ion pump from *Natronobacterium pharaonis.* In order to clarify the role of Ser-130$^{phR}$ residue which corresponds to Ser-115$^{shR}$ for *salinarum* hR on the anion-binding affinity, the wild-type and Ser-130 mutants substituted with Thr, Cys and Ala were expressed in *E. coli* cells and solubilized with 0.1% *n*-dodecyl β-D-maltopyranoside The absorption maximum ($\lambda_{max}$) of the S130T mutant indicated a blue shift from that of the wild type in the absence and presence of chloride. For S130A, a large red shift (12 nm) in the absence of chloride was observed. The wild-type and all mutants showed the blue-shift of $\lambda_{max}$ upon $Cl^-$ addition, from which the dissociation constants of $Cl^-$ were determined. The dissociation constants were 5, 89, 153 and 159 mM for the wild-type, S130A, S130T and S130C, respectively, at pH 7.0 and 25 °C. Circular dichroic spectra of the wild-type and the Ser-130 mutants exhibited an oligomerization. The present study revealed that the Ser-130 of *N. pharaonis* halorhodopsin is important for the chloride binding.
© 2003 Elsevier Science B.V. All rights reserved.

*Keywords:* Chloride binding; Chloride pump; Archaeal rhodopsin; Mutation

## 1. Introduction

Halorhodopsin (hR) has been discovered in the cytoplasmic membrane of *Halobacterium salinarum,* halophilic archaea, as an inward light-driven chloride pump [1–6], which generates the interior negative membrane potential on illumination. This generation of the membrane potential is considered to assist ATP synthesis done by bacteriorhodopsin (bR), an outward light-driven proton pump and by the respiratory chain [1]. Up to now, many hRs have been identified and reported [7–9], but only those from *H. salinarum* [10–17] and *Natronobacterium pharaonis* [18–23] have been extensively studied. In this paper, hR from *H. salinarum* is

*Abbreviations:* bR, Bacteriorhodopsin; DM, *n*-dodecyi β-D-maltopyranoside; *p*hR, Halorhodopsin from *Natronobacterium pharaonis*; *s*bR, Bacteriorhodopsin from *Halobacterium salinarum*; *s*hR, Halorhodopsin from *Halobacterium salinarum*.

*Corresponding author. Tel.: +81-11-706-2771; fax: +81-11-706-2771.

*E-mail address:* demura@sci.hokudai.ac.jp (M. Demura).

0301-4622/03/$ - see front matter © 2003 Elsevier Science B.V. All rights reserved.
PII: S0301-4622(02)00368-X

designated *s*hR and from *N. pharaonis* is designated as *p*hR.

The photocycle of *p*hR has intermediates analogous to bR. Spectral and kinetic studies have clarified the following photocycle of *p*hR: *p*hR → K ↔ L ↔ N ↔ O ↔ *p*hR′ [19,22]. In the case of *s*hR, the O-intermediate does not accumulate, presumably for kinetic reasons [14]. The release and uptake of $Cl^-$ are associated with the N to O and the O to hR′ reaction, respectively. Mutagenesis studies on *s*hR have revealed that the extracellular pair R108/T111$^{shR}$ plays an important role in the chloride uptake by increasing affinity of the $Cl^-$ binding, and that the cytoplasmic pair R200/T203$^{shR}$ was a candidate for the $Cl^-$ binding site concerning the release [12]. Furthermore, His-95$^{shR}$, which is located in the extracellular loop between helices B and C, is presumably an importance residue for the $Cl^-$ uptake [13]. However, the molecular event on the $Cl^-$ transport mechanism has not been elucidated.

The X-ray crystal structure of *s*hR was solved at 1.8 Å resolution, showing that a single $Cl^-$ ion next to the Schiff base nitrogen is closely associated with the isomerizable chromophore [24]. Fig. 1 shows the crystal structures of *s*hR and the alignment of primary structures of *p*hR and *s*hR. Chloride accepts hydrogen bonds only from two-bound water (3.14 and 3.21 Å) and Ser-115$^{shR}$ (3.07 Å). Therefore, Ser-115$^{shR}$ that is connected with hydrogen bonds to $Cl^-$ in the ground state might be instrumental to keep the chloride solvated in the internal cavity; i.e. it is anticipated that Ser-115$^{shR}$ plays an important role in the anion binding and the structure of the bound water.

What residue(s) are important for $Cl^-$ binding of *p*hR? The X-ray structure of *p*hR has not been solved yet and the $Cl^-$ binding site is not clarified. Since the primary structures of the *salinarum* hR and *pharaonis* hR are very highly homologous (66%) [25], the most plausible candidate is Ser-130 of *p*hR which corresponds to Ser-l15$^{shR}$. We expressed histidine-tagged wild-type *p*hR and Ser-130 point mutants in *Escherichia coli* cells to investigate the affinity for $Cl^-$. It is concluded that Ser-130$^{phR}$ in helix C is one of the essential residues for the chloride binding.

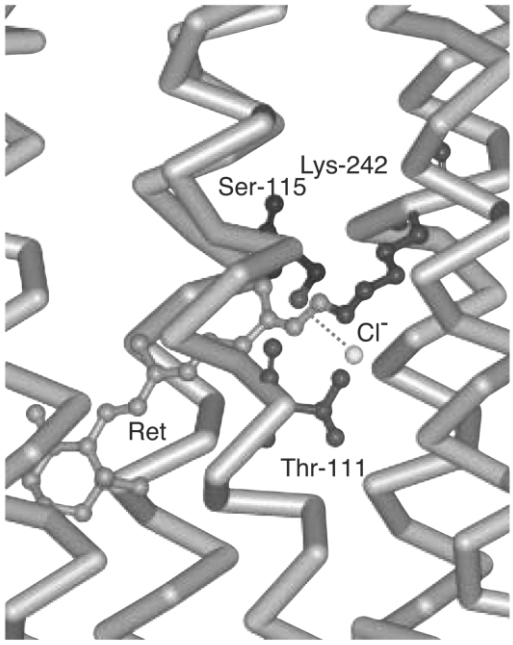


phR (115–142)
DG**V**VTM**WGRYLTWAL**[**S**]**TPMILLALGLLA**
shR (100–127)
EM**V**RSQ**WGRYLTWAL**[**S**]**TPMILLALGLLA**

Fig. 1. Structure of the Schiffbase region in *s*hR (PDB code: 1E12) [24] (upper). A number of key residues in the retinal binding pocket are shown. The membrane normal is approximately in the vertical direction of these figures. Ret denotes the all-*trans* retinylidene chromophore. The dotted line represents the hydrogen bond. The sequence homologies of *p*hR and *s*hR are given in (lower). Partial amino acid residues are shown only for the helix-C region. Bold and underlined letters indicate conserved amino acid residues among those of *p*hR. Squared letters of *p*hR and *s*hR correspond to Ser-130 and Ser-115, respectively.

## 2. Materials and methods

### *2.1. Construction of expression plasmids of S130 mutants having the histidine-tag*

Mutant plasmids for the expression of Ser130$^{phR}$ mutant substituted with Ala (S130A), Cys (S130C) and Thr (S130T) were constructed with a Quikchange Site-Directed Mutagenesis Kit (Stratagene Cloning Systems, La Jolla, CA) and

the modified pET-21c(+) vector to utilize the histidine-tagged region [18,26,27]. The sequences of the primers designated to replace the Ser130 codon with other ammo acid codons were 5′-G ACG TGG GCC CTT GCG (for Ala)/TGC (for Cys)/ACG (for Thr) ACA CCG ATG ATA C-3′ and 5′-G TAT CAT CGG TGT CGC (for Ala)/ ACG (for Cys)/TGC (for Thr) AAG GGC CCA CGT C-3′. The mutations introduced into the plasmid were confirmed by DNA sequencing using a DNA sequencing kit (Applied Biosystems, Foster City, CA), and each mutated plasmid was introduced into BL21(DE3) cells. Transformed cells were selected by their ampicillin resistance.

### 2.2. Protein expression and purification of phR

The protein expression and purification procedures using *E. coli* BL21(DE3) cells harboring the plasmid were described in detail in a previous paper [18]. Fractions of the proteins using Ni–NTA agarose (Qiagen, Hilden, Germany) were collected by elution (flow rate, 56 ml/h) with buffer E (50 mM Tris–HCl (pH 7.0), 300 mM NaCl, 150 mM imidazole and 0.1% *n*-dodecyl β-D-maltopyranoside (dodecylmaltoside, DM) (Dojindo Lab, Kumamoto, Japan).

### 2.3. Preparation of the $Cl^-$ free species

Anion-depleted red-shifted species of the wild-type and the mutants were prepared by interchanging with buffer C (10 mM 2-morpholinopropanesulfonic acid, MOPS (pH 7.0) and 0.1% DM) by passing over a Sephadex-025 column (2.5×20 cm; Amersham Pharmacia Biotech, Uppsala, Sweden) at a flow rate of 2 ml/min. After the buffer exchange, the protein concentration was estimated using an excitation coefficient $\varepsilon_{600}$ of 50 000 $M^{-1}$ $cm^{-1}$ [28]. The anion-depleted species of S130A and S130C were used immediately after the preparation (within 5 h) to avoid denaturing.

### 2.4. Absorption and circular dichroic measurements

Circular dichroic (CD) spectra of the wild-type and the mutants were measured with a Jasco J-725 spectropolarimeter (Jasco, Tokyo, Japan) in the 300–750 nm region at 25 °C using a scanning speed of 200 nm/min and two-times accumulations. The measuring medium was buffer C containing various concentrations of NaCl. The protein concentration was 18 μM. The path-length of the optical cuvette was 10 mm. Absorption spectra were obtained by converting a photomultiplier voltage signal of a CD apparatus into the optical density ($\log I_0/I$) using a computer.

## 3. Results and discussion

### 3.1. Expression and purification of the wild-type and mutant proteins

The wild-type *p*hR and Ser-130 mutants (S130A, S130C and S130T) were expressed heterologously in *E. coli*. All mutants were solubilized with DM and purified with NTA resins. The yield of S130T was nearly equal to that of the wild-type *p*hR, but the yields of S130A and S130C were very low compared with that of the wild-type (30% for S130A and 50% for S130C), if extinction coefficients for the mutants were assumed identical to that of the wild-type. As shown in Fig. 2, the CD spectra show the small positive band near 400 nm for S130A and S130C which may come from another conformation, but the wild-type and S130T have little at 400 nm. Similar additional absorption at 390 nm (Fig. 3) of the S130A and S130C mutants was observed. In addition, S130A and S130C lost their color gradually over 1 week when stored even in cool. Removal of $Cl^-$ by the buffer exchange (for composition, see Section 2) facilitated the bleaching. The buffer composition did not contain a high concentration of salt, and then the bleaching was checked in 1 M $Na_2SO_4$. The high salt concentration did not rescue the bleaching. On the other hand, the wild-type and S130T did not lose their color in the presence or absence of CT as well as in a dilute salt solution. These findings suggest the importance of an OH-residue of Ser or Thr at this position for the maintenance of the structure. The binding of $Cl^-$ might partially strengthen the structure. Hence, the experiments were performed as quickly as possible, as was mentioned in the experimental section.

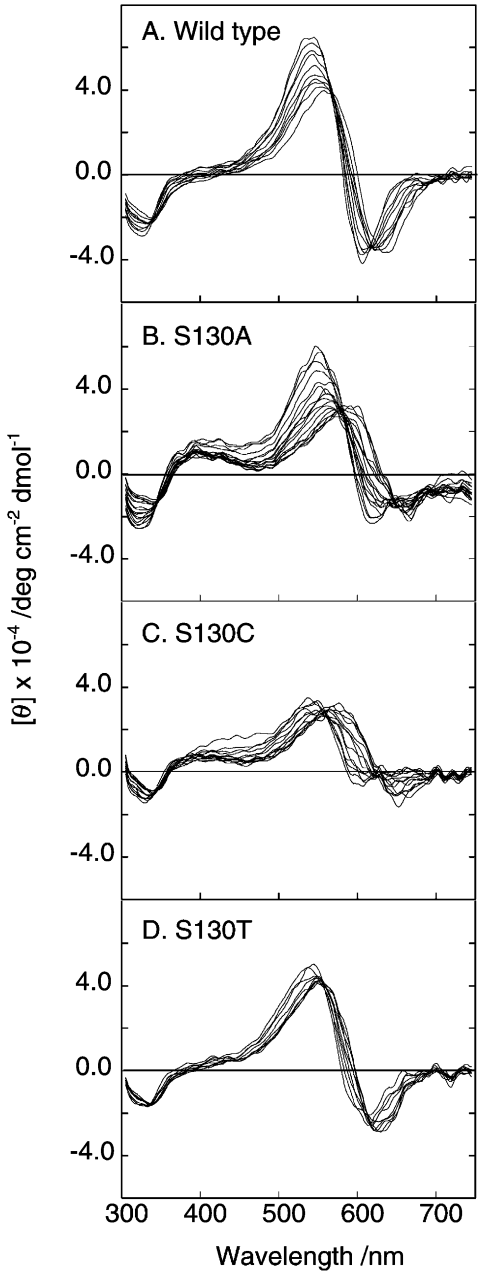


Fig. 2. Circular dichroic spectra of the wild-type *p*hR and Ser-130 mutants at various $Cl^-$ concentrations. The pigment protein of 18 μm was suspended in 10 mM MOPS (pH 7.0) and 0.1% DM. NaCl was added at a concentration of 0–1 M; these concentrations are indicated in the abscissa in Fig. 4. The volume changes due to the addition of the concentrated NaCl solutions were corrected. The measurement was carried out at 25 °C.

### *3.2. Titration of the wild-type and mutants with chloride on visible CD and absorption spectra*

The $Cl^-$-free blue forms of the wild-type and Ser-130*p*hR mutants were titrated with NaCl. Each circular dichroic (CD) spectrum in the visible region (450–700 nm) exhibited a bilobe (see Fig. 2) as well as previous reports [18,28]. Here the CF concentration ranged from 0 to 1 M. From CD spectroscopic studies of bR, a bilobe in the visible region is interpreted as a superposition of the following two components: (1) symmetrical positive and negative bands arising from the excitonic interaction between chromophores of neighboring molecules (exciton band); and (2) a positive band originated from the retinal pocket with its own asymmetric protein environment [29–31]. Therefore, this figure indicates that the Ser-130*p*hR mutants have the excitonic interaction between chromophores of neighboring molecules as well as the wild-type. In the case of the $Cl^-$-free condition, the exciton band of the CD spectrum of the wild-type is symmetrical with respect to the crossover point of the bilobe, but Ser-130 mutants, particularly S130C, are asymmetrical. The negative band of S130C is very small compared with that of the other samples. In the case of the wild-type and S130A, crossover points are blue-shifted and the positive exciton bands are gradually increased with increasing $Cl^-$ concentration, and S130T showed similar tendency with small changes. On the other hand, only in S130C, the blue shift of the bilobe was observed, and no increase in the positive band was observed with increasing chloride concentration. The reason for this finding is not clear, but it might be associated with the lowest affinity of the chloride ion (Table 1).

Fig. 3 shows absorption spectra in the range of 300–750 nm when titrated with $Cl^-$ from 0 to 1 M at pH 7.0. In the absence of $Cl^-$, S130C had the same absorption maximum, $\lambda_{max}$, as the wild-type, whereas the replacement by Ala and Thr caused the red and blue shifts of 11–12 nm, respectively (Table 1). The absorption maxima of all mutants were blue-shifted with an increase in the $Cl^-$ concentration (Fig. 3). S130A showed a large shift by 30 nm, whereas S130T showed a small shift by 16 nm. The isosbestic point of the

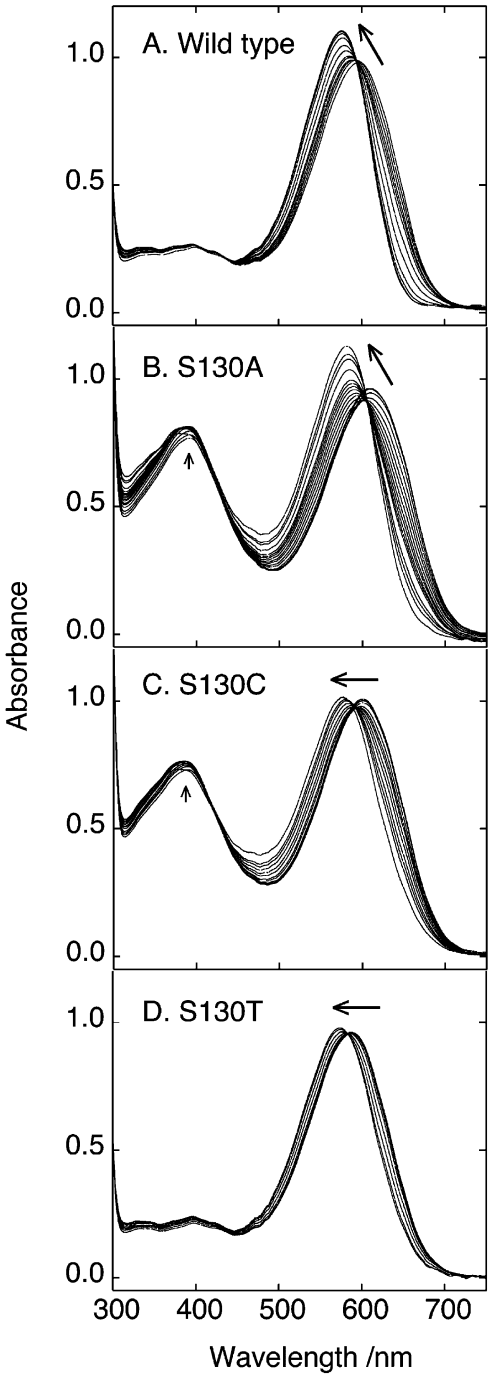


Fig. 3. Absorption spectrum changes caused by the reaction from the $Cl^-$-free form to $Cl^-$-bound form. The experimental conditions are the same as in Fig. 2. Arrows indicate the increasing $Cl^-$ concentration.

wild-type and S130C were 590 nm, but those of S130A and S130T were 604 and 583 nm, respectively.

Fig. 4 shows the shift of the wavelength in the absorption maximum ($\Delta\lambda_{max}$) as a function of $Cl^-$-concentration at pH 7.0. Upon addition of CF to Ser-130 mutants, the shifts followed sigmoidal curves with saturation similar to the wild-type. The values of $\Delta\lambda_{max}$ were normalized by the saturation level. This shift comes from the $Cl^-$ binding near the Schiff base [28]. The apparent half-maximal binding concentration increased in the order of the wild type < S130A < S130C and S130T. These saturation curves were fitted with the following equation:

$$\Delta\lambda_{max} = [\text{chloride}]^n/(K_d^n + [\text{chloride}]^n),$$

where $K_d$ and $n$ are the dissociation constant and Hill coefficient, respectively. The results are listed in Table 1. Values of $K_d$ for the wild-type, S130A, S130C and S130T were 6, 89, 159 and 153 mM, respectively. The Hill coefficient for the wild-type was approximately 1, but those for the Ser-130 mutants were much larger than unity. The difference of Hill coefficient between the wild-type and mutants might originate from the induced structural change. Another possibility might be the presence of several $Cl^-$ binding sites with weak affinities in the mutants.

Absorbance changes (not the $\lambda_{max}$ shift as in Fig. 4) at respective wavelengths (635, 646, 633 and 624 nm for the wild-type, S130A, S130C and S130T, respectively), were analyzed with the Hill-equation, where the wavelengths were chosen so as to obtain the largest values. The selected wavelength was different for the wild-type and mutants because their $\lambda_{max}$'s differ from one another. The data, unfortunately, failed to fit well, but the order of the affinity for the $Cl^-$ binding was the same as listed in Table 1. Therefore, aside from the quantitative estimation, the order of the binding affinity is certainly as follows: wild-type > S130 > S130C, S130T. Replacing Asp-$85^{bR}$, which corresponds to Thr-$111^{shR}$, with Thr converting bR from a proton pump into a chloride ion pump [32]. The dissociation constant of the $D85T^{bR}$ mutant measured in 50 mM citrate (pH 5) was reported to be

Table 1
Dissociation constants ($K_d$), Hill coefficients ($n$), absorption maxima ($\lambda_{max}$) and opsin shifts ($\Delta\nu$) of the $Cl^-$-free and $Cl^-$-bound forms of various *p*hR mutants at pH 7.0 and 25 °C

| Opsin type | $K_d$/mM | $n$ | NaCl-free | | 1 M NaCl | |
|---|---|---|---|---|---|---|
| | | | $\lambda_{max}$/nm | $\Delta\nu$/cm$^{-1}$ | $\lambda_{max}$/mn | $\Delta\nu$/cm$^{-1}$ |
| Wild-type | 5 | 1.0 | 599 | – | 577 | – |
| S130A | 89 | 1.7 | 611 | −328 | 583 | −119 |
| S130C | 159 | 1.9 | 600 | −28 | 577 | 0 |
| S130T | 153 | 2.0 | 588 | 312 | 572 | 151 |

The dissociation constant and Hill coefficient were determined from the equation shown in text by least-square fits. $\Delta\nu$ is the opsin shift value from wild-type *p*hR.

221 mM by Paula et al. [33]. In the present study, the $Cl^-$ affinities observed for S130T might be allowed to be considered as equal to that for the $D85T^{bR}$ mutant (note that $D85T^{bR}$ has a sequence of $T^{85}$WLFT while the corresponding sequence is $TWALT^{130}$ for S130T *p*hR mutant). This coincidence might suggest that the *p*hR mutants, S130T have similar environments to $D85T^{bR}$ in the chromophore region. Further detailed studies are needed on the characteristic relationship between the visible absorption and molecular structure of *p*hR in the presence and absence of $Cl^-$.

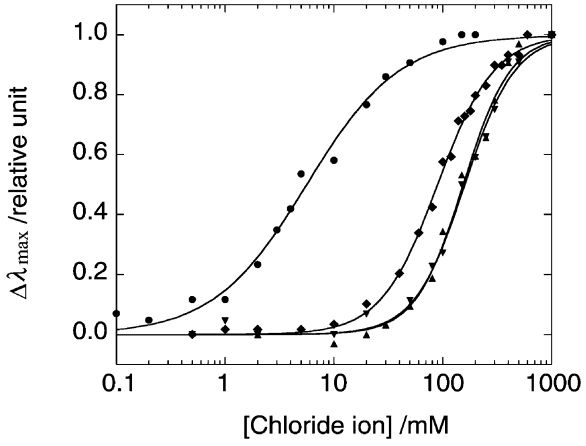


Fig. 4. The absorption maximum changes vs. salt concentrations during the reaction from the $Cl^-$-free form to the $Cl^-$-bound form. The ordinate value was reduced by the maximum absorption changes of the respective protein, ●,wild-type; ♦, S130A; ▲, S130C; ▼, S130T. The samples of the $Cl^-$-free form (18 μM) were solubilized in 10 mM MOPS (pH 7.0) and 0.1% DM, followed by the addition of chloride. The solid lines are the best-fitted results using the equation described in Section 3.

## 4. Conclusions

The wild-type *p*hR and the Ser-130 mutants substituted by Thr, Cys and Ala showed differing levels of chloride accessibility. Replacement of Ser-130 reduces greatly the $Cl^-$-binding affinity. The results obtained here indicated that the Ser residue at position 130 of *p*hR is one of the essential residues for the chloride binding. As is the same as *s*hR, this Ser residue may contact the chloride ion in the retinal pocket. The direct evidence may be obtained from the X-ray structure that might be obtained in future.

## Acknowledgments

The authors are very grateful to Dr Y. Imamoto for useful discussion and to M. Iwamoto and Y. Sudo for their invaluable advice.

## References

[1] A. Matsuno-Yagi, Y. Mukohata, ATP synthesis linked to light-dependent proton uptake in a red mutant strain of Halobacterium lacking bacteriorhodopsin, Arch. Biochem. Biophys. 199 (1980) 297–303.
[2] B. Schobert, J.K. Lanyi, Halorhodopsin is a light-driven chloride pump, J. Biol. Chem. 257 (1982) 10306–10313.
[3] L.O. Essen, Halorhodopsin: light-driven ion pumping made simple?, Current Opin. Struct. Biol. 12 (2002) 516–522.

[4] G. Varo, Analogies between halorhodopsin and bacteriorhodopsin, Biophys. Biochem. Acta 1460 (2000) 220–229.
[5] D. Oesterhelt, Structure and function of halorhodopsin, Israel J. Chem. 35 (1995) 475–494.
[6] J.K. Lanyi, Halorhodopsin, a light-driven electrogenic chloride-transport system, Physiol. Rev. 70 (1990) 319–330.
[7] J. Otomo, H. Tomioka, H. Sasabe, Properties and the primary structure of a new halorhodopsin from halobacterial strain mex, Biochim. Biophys. Acta 1112 (1992) 7–13.
[8] J. Soppa, J. Duschi, D. Oesterhelt, Bacterioopsin, halorhodopsin, and sensory opsin I of the halobacterial isolate Halobacterium sp, strain SG 1: three new members of a growing family, J. Bacterial. 175 (1993) 2720–2726.
[9] K. Ihara, T. Umemura, I. Katagiri, T. Kitajima-Ihara, Y. Sugiyama, Y. Kimura, et al., Evolution of the archaeal rhodopsins: evolution rate changes by gene duplication and functional differentiation, J. Mol. Biol. 285 (1999) 163–174.
[10] M.S. Hutson, S.K. Shilov, R. Krebs, M.S. Braiman, Halide dependence of the halorhodopsin photocycle as measured by time-resolved infrared spectra, Biophys. J. 80 (2001) 1452–1465.
[11] Y.S. Chon, H. Kandori, J. Sasaki, J.K. Lanyi, R. Needleman, A. Maeda, Existence of two L photointermediates of halorhodopsin from Halobacterium salinarum, differing in their protein and water FTIR bands, Biochemistry 38 (1999) 9449–9455.
[12] M. Rüdiger, D. Oesterhelt, Specific arginine and threonine residues control anion binding and transport in the light-driven chloride pump halorhodopsin, EMBO J. 16 (1997) 3813–3821.
[13] J. Otomo, Influence exercised by hisddine-95 on chloride transport and the photocycle, Biochemisty 35 (1996) 6684–6689.
[14] G. Váró, L. Zimanyi, X.L. Fan, L. Sun, R. Needleman, J.K. Lanyi, Photocycle of halorhodopsin from *Halobacterium salinarum*, Biophys. J. 68 (1995) 2062–2072.
[15] M. Rudiger, U. Haupts, K. Gerwert, D. Oesterhelt, Chemical reconstitution of a chloride pump inactivated by a single point mutation, EMBO J. 14 (1995) 1599–1606.
[16] R.A. Bogomoini, M.E. Taylor, W. Stoeckenius, Reconstitution of purified halorhodopsin, Proc. Nat. Acad. Sci. USA 81 (1984) 5408–5411.
[17] N. Kamo, N. Hazemoto, Y. Kobatake, Y. Mukohata, Light and dark adaptation of halorhodopsin, Arch. Biochem. Biophys. 238 (1985) 90–96.
[18] T. Sato, M. Kanamori, N. Kamo, M. Demura, K. Nitta, Stopped-flow analysis on anionbinding to blue-form halorhodopsin from Natronobacterium pharaonis: comparison with the anion-uptake process during the photocycle, Biochemistry 41 (2002) 2452–2458.
[19] I. Chizhov, M. Engelhard, Temperature and halide dependence of the photocycle of halorhodopsin from *Natronobacterium pharaonis*, Biophys. J. 81 (2001) 1600–1612.
[20] C. Hackmann, J. Guijarro, I. Chizhov, M. Engelhard, C. Rodig, F. Siebert, Static and time-resolved step-scan Fourier transform infrared investigations of the photoreaction of halorhodopsin from *Natronobacterium pharaonis*: consequences for models of the anion translocation mechanism, Biophys. J. 81 (2001) 394–406.
[21] S. Gerscher, M. Mylrajan, P. Hildebrandt, M.H. Barton, R. Muller, M. Engelhard, Chromophore-anion interactions in halorhodopsin from *Natronobacterium pharaonis* probed by time-resolved resonance Raman, Biochemistry 36 (1997) 11012–11020.
[22] G. Váró, L.S. Brown, J. Sasaki, H. Kandori, A. Maeda, R. Needleman, et al., Light-driven chloride ion transport by halorhodopsin from Natronobacterium pharaonis. 1. The photochemical cycle, Biochemistry 34 (1995) 14490–14499.
[23] G. Varo, R. Needleman, J.K. Lanyi, Light-driven chloride ion transport by halorhodopsin from Natronobacterium pharaonis. 2. Chloride release and uptake, protein conformation change, and thermodynamics, Biochemistry 34 (1995) 14500–14507.
[24] M. Kolbe, H. Besir, L.O. Essen, D. Oesterhelt, Structure of the light-driven chloride pump halorhodopsin at 1.8 Å resolution, Science 288 (2000) 1390–1396.
[25] A. Duschi, J.K. Lanyi, L. Zimanyi, Properties and photochemistry of a halorhodopsin from the haloalkalophile, *Natronobacterium pharaonis*, J. Biol. Chem. 265 (1990) 1261–1267.
[26] K. Shimono, M. Iwamoto, M. Sumi, N. Kamo, Functional expression of pharaonis phoborhodopsin in *Escherichia coli*, FEBS Lett. 420 (1997) 54–56.
[27] I.P. Hohenfeld, A.A. Wegener, M. Engelhard, Purification of histidine tagged bacteriorhodopsin, pharaonis halorhodopsin and pharaonis sensory rhodopsin II functionally expressed in *Escherichia coli*, FEBS Lett. 442 (1999) 198–202.
[28] B. Scharf, M. Engelhard, Blue halorhodopsin from *Natronobacterium pharaonis*: wavelength regulation by anions, Biochemistry 33 (1994) 6387–6393.
[29] M.P. Heyn, P.J. Bauer, N.A. Dencher, A natural CD label to probe the structure of the purple membrane from halobacterium halobium by means of exciton coupling effect, Biochem. Biophys. Res. Commun. 67 (1975) 897–903.
[30] B. Becher, T.G. Ebrey, Evidence for chromophore-chromophore (exciton) interaction in the purple membrane of *Halobacterium halobium*, Biochem. Biophys. Res. Commun. 69 (1976) 1–6.
[31] T.G. Ebrey, B. Becher, B. Mao, P. Kilbride, B. Honig, Exciton interactions and chromophore orientation in the purple membrane, J. Mol. Biol. 112 (1977) 377–397.

[32] J. Sasaki, L.S. Brown, Y.-S. Chon, H. Kandori, A. Maeda, R. Needleman, et al., Conversion of bacteriorhodopsin into a chloride ion pump, Science 26 (1995) 73–75.

[33] S. Paula, J. Tittor, D. Oesterhelt, Roles of cytoplasmic arginine and threonine in chloride transport by the bacteriorhodopsin mutant D85T, Biophys. J. 80 (2001) 2386–2395.